



OPEN Regenerative effect of lyophilized dental follicle mesenchymal stem cells and platelet-rich fibrin in skin wounds in geriatric and young rats

Osman Bulut¹✉, Deniz Genç^{2,3}, Çiğdem Elif Demirci³, Leyla Tekin⁴, Tolga Meriç Dömbek¹ & Aziz Bülbül⁵

The aim of this study was to investigate the regenerative effect of lyophilized dental follicle mesenchymal stem cells (DF-MSCs) combined with rat platelet-rich fibrin (PRF) on geriatric skin wounds. Human DF-MSCs which were isolated from the wisdom teeth of healthy donors and PRF were mixed and incubated in a 37 °C incubator for 1–2 h containing 1 million cells in 150 mg PRF. The mixture was suspended in a freeze-drying solution and then lyophilized. Wounds were created on the back skin of Wistar albino rats using a 6 mm punch. Lyophilized DF-MSCs, PRF, or PRF + DF-MSCs were applied to the wounds of rats. On the 15th day, the wound area was histopathologically evaluated in rats. Blood samples from rats were analyzed for total antioxidant status (TAOS), and inflammatory cytokine levels using ELISA. In both young and geriatric rats treated with lyophilized PRF + DF-MSCs, wound area began to significantly decrease from the 10th day compared to the untreated group ($p < 0.05$). Histopathological examination revealed that in the lyophilized PRF + DF-MSCs treated groups, epithelial integrity and scarless healing significantly increased compared to the untreated groups ($p < 0.05$). There were no significant differences in TAOS, total oxidant status (TOS), tumor necrosis factor (TNF), interleukin-6 (IL6), and hydroxyproline levels in serum samples from young rats on the 15th day. In geriatric rats, hydroxyproline (HYP) levels were increased in the DF-MSC and PRF + DF-MSC groups ($p < 0.01$), TNF was significantly elevated in PRF geriatric group and IL6 was increased in the PRF group compared to the control group ($p = 0.01$). Lyophilized PRF + DF-MSCs, which is a shelf-stable and ready-to-use product, hold promise, especially for traumatic wounds in geriatric individuals with longer healing times.

Keywords Lyophilized mesenchymal stem cells, Lyophilized platelet-rich fibrin, Skin wounds

Abbreviations

DF-MSCs	Dental follicle mesenchymal stem cells
PRF	Platelet-rich fibrin
TAOS	Total antioxidant status
TOS	Total oxidant status
TNF	Tumor necrosis factor
IL-6	interleukin-6
PDGF	Platelet-derived growth factor
MSC	Mesenchymal stem cells
FGF	Fibroblastic growth factor
VGEF	Vascular endothelial growth factor
IGF	Insulin-like growth factor
TGF- β	Transforming growth factor beta
EGF	Epidermal growth factor

¹Department of Surgery, Faculty of Milas Veterinary Medicine, Muğla Sıtkı Kocman University, Milas, Mugla, Turkey.

²Department of Pediatric Diseases, Faculty of Health Sciences, Muğla Sıtkı Kocman University, Mugla, Turkey. ³The Center of Research Laboratories, Muğla Sıtkı Kocman University, Mugla, Turkey. ⁴Faculty of Medicine, Department of Pathology, Mugla Sıtkı Kocman University, Mugla, Turkey. ⁵Department of Physiology, Faculty of Milas Veterinary Medicine, Muğla Sıtkı Kocman University, Milas, Mugla, Turkey. ✉email: obulut@mu.edu.tr

PDEGF	Platelet-derived epidermal growth factor
PDAF	Platelet-derived angiogenesis factor
PF-4	Platelet factor 4
PVP40	Polyvinylpyrrolidone 40
DMEM	Dulbecco's modified eagle medium
FBS	Fetal bovine serum
PBS	Phosphate buffer solution
CO ₂	Carbon dioxide
MFI	Mean fluorescent intensity
SEM	Scanning electron microscope
HYPR	Hydroxyproline
ROS	Reactive oxygen species

A wound is the loss of anatomical structure and function of living tissue due to various reasons, resulting in a temporary loss of all or part of its existing biological and physical properties¹. Studies have determined that the response of wound endothelial cells to platelet-derived growth factor (PDGF) stimulation in geriatric animals is less than that in young animals. It has been found that collagen synthesis and epithelialization in the wound area decrease with age².

Mesenchymal Stem Cells (MSC) are multipotent stromal cells of mesodermal origin that can self-renew, regulate immune responses, and differentiate into other tissue cells³. MSC also expedites the tissue regeneration process by secreting growth factors such as fibroblastic growth factor (FGF), vascular endothelial growth factor (VEGF), and insulin-like growth factor (IGF)⁴. Among them, dental MSCs are potent candidates for the treatment of inflammatory diseases due to their easily accessible source, ease of isolation, rapid proliferation in culture, multipotent differentiation ability, and high immunomodulatory effects⁵. Dental follicle progenitor/stem cells (DF-MSCs) have a multipotent differentiation capacity that resides in the dental follicle and originates from the neural crest. More importantly, compared to other stem cells, they have advantages such as abundance of cell number, active self-renewal ability and multiple differentiation capability, making them an attractive candidate in the field of tissue engineering^{4,5}.

Platelet-rich fibrin (PRF) is a fibrin matrix that supports wound healing, bone regeneration, graft stabilization, and hemostasis⁶. PRF creates a supportive microenvironment for wounds as it contains PDGF, transforming growth factor beta (TGF- β), epidermal growth factor (EGF), VEGF, IGF, platelet-derived epidermal growth factor (PDEGF), platelet-derived angiogenesis factor (PDAF), and platelet factor 4 (PF-4)⁷.

Many studies to date have demonstrated the regenerative effects of fresh PRF or MSCs on skin wounds, musculoskeletal injuries, and bone wounds^{8–10}. Additionally, the study has shown that lyophilized PRF can accelerate the healing process of wounds, similar to fresh-prepared PRF¹¹. Few studies have demonstrated the effect of lyophilized MSCs on wound healing. In one study, researchers concluded that lyophilized MSCs provided hemostasis without creating a thrombus after anastomosis¹². Recent studies have focused on cell-based therapies that are easy to apply. In the present study, we developed a novel method for lyophilization of MSCs with PRF. The lyophilization solution contains trehalose, and PVP40 (Polyvinylpyrrolidone 40) which are combined with the cells suspension in PRF. This method for lyophilization increased the viability and preserved the differentiation ability of MSCs.

In this study, we investigated the regenerative effects of lyophilized DF-MSCs, which were isolated from healthy individuals, combined with rat PRF as a new therapeutic product on deep skin wounds in geriatric rats with very slow healing processes. In the present study, rat PRF was used to avoid a hypersensitivity reaction between species since it would be used in wounds created in rats. We also compared the wound healing results of geriatric rats with those of young rats. The content of the lyophilization solution combined with PRF we used in this study consists of ingredients we developed specifically to ensure that MSCs have a long shelf life in a powder form.

Materials and methods

Ethics approval and consent to participate

Ethical approval was obtained from the ethics committee of Mugla Sıtkı Koçman University (Project title: Regenerative Effect of Lyophilized Mesenchymal Stem Cells Combined with Platelet-Rich Fibrin in a Skin Wound Model in Geriatric and Young Rats; Approval no. 39/22; Date of approval: 18/08/2022). In the study, DF-MSCs were obtained from humans (19–24 years old) with an orthodontic indication for wisdom tooth extraction, and informed consent forms were signed. This study was conducted and reported in accordance with the ARRIVE guidelines. All methods were carried out in accordance with relevant guidelines and regulations.

Animals and wound creation

Thirty-six male Wistar albino rats aged 3–6 months (250–400 g) were classified as young rats, while thirty-six male rats aged 18–24 months were classified as geriatric rats. The rats were housed under a 12/12-hour light/dark cycle at a temperature of 22 ± 2 °C, with ad libitum water and food. The Mugla Sıtkı Koçman University Experimental Animals Application and Research Center provided the rats and the experimental phase was conducted at this center. The sample size was calculated using the G-Power program, considering an effect size (0.50), a type-I error (0.05) and power (0.80) for eight groups ($n=9$).

The rats were divided into eight groups as follows: Group 1: Geriatric Wound, Group 2: Young Wound, Group 3: Geriatric Wound+lyophilized PRF (in a powder form), Group 4: Young Wound+lyophilized PRF (in a powder form), Group 5: Geriatric Wound+lyophilized MSCs (in a powder form), Group 6: Young Wound+lyophilized MSCs (in a powder form), Group 7: Geriatric Wound+lyophilized PRF+MSCs (in a powder form), Group 8: Young

Wound + lyophilized PRF + MSCs (in a powder form). Anesthesia was administered by intraperitoneal injection of 10 mg/kg Xylazine hydrochloride (Rompun, Bayer 23.32 mg/mL) followed by intraperitoneal injection of 70 mg/kg Ketamine hydrochloride (Ketalar, Parke-Davis, 50 mg/mL). Rats' backs were shaved, cleaned with povidone-iodine, and a 6 mm punch created a full-thickness skin wound (1 mm depth). Post surgery, 10 mg/kg Enrofloxacin (Baytril, Bavet, 100 mg/mL) and 5 mg/kg Carprofen (Rimadyl, Zoetis, 50 mg/mL) were administered for 3 days to manage infection and pain. Euthanasia was performed 15 days post wounding by cervical dislocation under anesthesia.

Production and characterization of DF-MSCs

Human DF-MSCs which previously obtained from Muğla Sıtkı Koçman University Hospital of Dentistry, in the stocks of Muğla Sıtkı Koçman University Stem Cell Laboratory, were cultured at the third passage with Dulbecco's Modified Eagle Medium (DMEM) (Gibco, Cat.No: 11885084, USA) supplemented with 10% fetal bovine serum (FBS) (Sigma, Cat.No: F6765, USA) and 1% penicillin/streptomycin (10,000 U/mL, 10,000 µg/mL) (Gibco, Cat.No: 15140122, USA) until reaching 80–90% confluence. After the detachment of the cells with 0.25% trypsin-EDTA (Sigma, Cat.No: SM-2003, USA), cells were washed two times with phosphate buffer solution (PBS) (Millipore, Cat.No: 524650, USA). The cell pellet was obtained after centrifugation at 1200 rpm for 5 min. The cell pellet was immediately used to prepare PRF and MSC combination.

100,000 cells were subjected to characterization analyses via flow cytometry. Cells were analyzed for the positive markers for MSCs by staining with anti-CD29 (BD Pharmingen, Cat.No: 556049, USA), anti-CD73 (BD Pharmingen, Cat.No: 560847), anti-CD105 (BD Pharmingen, Cat.No: 561443, USA), and anti-CD90 (BD Pharmingen, Cat.No: 561557, USA) and negative markers for MSCs by staining with anti-CD14 (BD Pharmingen, Cat.No: 562691, USA), anti-CD45 (BD Pharmingen, Cat.No: 564105, USA), anti-CD34 (BD Pharmingen, Cat.No: 340441, USA), and anti-HLADR (BD Pharmingen, Cat.No: 560944, USA).

DF-MSCs in the third passage were subjected to osteogenic, chondrogenic, and adipogenic differentiation assays to prove that they had MSCs characteristics. In brief, the third passage cells were incubated in 6-well plates for 48 h (2×10^5 cells/well) at 37 °C in a humidified chamber. After 48 h of incubation period cells were cultured separately with Osteogenic Differentiation Medium (Gibco, StemPro™, Cat.No: A1007201, USA), or Chondrogenic Differentiation Medium (Gibco, StemPro™, Cat.No: A1007101, USA), or Adipogenic Differentiation Medium (Gibco, StemPro™, Cat.No: A1007001, USA) for 14–21 days. At the end of the culture period, culture supernatants were removed and the cells were stained with Alizarin Red S (Sigma, Cat.No: A5533, USA) for calcium deposits for osteogenic differentiation, Alcian Blue (Sigma, Cat.No: A5268, USA) for proteoglycans for chondrogenic differentiation, and Oil Red O (Sigma, Cat.No: O1391, USA) for lipid droplets for adipogenic differentiation.

Fluorescent labeling of DF-MSCs

To analyze whether DF-MSC differentiated into epithelial cells in the wound tissue after the application of PRF + MSCs in the experimental wound model, the cells were labeled with the Qdot labeling kit (Qtracker® 655 Cell Labeling Kit, Thermofisher, Cat.No: Q25029, USA). In summary, after the DF-MSC at the third passage, were suspended in DMEM containing 10% FBS and 5 nmol/L Qdot for each 1×10^6 cell and incubated for 1 h at 37 °C in a 5% carbon dioxide (CO₂) chamber. For analysis, 10,000 MSCs were separated from the cells and analyzed in the FL3 channel of the flow cytometry device (BD Accuri C6 Plus, USA) for Qdot signaling. The data was expressed as mean fluorescent intensity (MFI).

Isolation of platelet-rich fibrin

PRF was isolated from cardiac puncture of rats as described previously¹³. Blood was taken from 15 male Wistar rats, aged 6–12 months and weighing 220 gr–420 gr, under general anesthesia with a 10–12 ml cardiac puncture. Briefly, whole blood samples were collected in 15 mL falcon tubes and centrifuged at 3000 rpm for 12 min. PRF was collected from the bottom fraction of centrifuged blood. The fresh PRF was analyzed for platelet count and growth factors, and the lyophilized PRF was analyzed for growth factors using flow cytometry.

Lyophilization of DF-MSCs and PRF

The lyophilization process of DF-MSCs or PRF was conducted as previously described^{7,14}. Briefly, MSCs (1×10^6 cells) were mixed with 100 mM trehalose and 30% PVP40 in a total volume of 1 mL. The cell suspension was frozen at -80 °C before lyophilization. Fresh PRF was directly frozen at -80 °C before the lyophilization process. The fabrication of lyophilized PRF with DF-MSCs was done as previously described with some modifications. Briefly, freshly prepared DF-MSCs (1×10^6 cells) were transferred to 150 mg of fresh PRF and mixed with a tissue mixer for 5 min at 37 °C. Then the PRF and cell mixture was incubated at 37 °C in a 5% CO₂ incubator for 1–2 h. PRF containing DF-MSCs were transferred to a 15 mL sterile falcon tube and the volume was completed to 1 mL with 100 mM trehalose (Millipore, Cat.No: 625625, USA) containing 30% PVP40 (Sigma, Cat.No: P0930, USA). The mixture was then frozen at -80 °C until lyophilization. MSCs, PRF or PRF with MSCs were subjected to a lyophilization process at -100 °C between 2 and 5 Pa for 24 h (Yamato DC-801 Freezer Dryer, Japan). The scanning electron microscope (SEM) (ZEISS, EVO LS10, Germany) images of lyophilized MSCs, PRF, and MSCs combined with PRF are shown in Fig. 1a.

Cell survival analysis after lyophilization

DF-MSCs were analyzed for cell survival after the lyophilization process before animal experiments. The survival analysis of DF-MSCs were performed as previously described with some modifications¹⁴. For the cell survival analysis, lyophilized DF-MSCs or DF-MSCs in PRF was diluted with DMEM supplemented with 20% FBS. After one hours of incubation period, cells were washed with PBS and the pellet was stained with Annexin V-7AAD antibodies, each 5 µL in a 100 µL staining buffer (BD Pharmingen, Cat.No: 559763, USA), for the cell survival

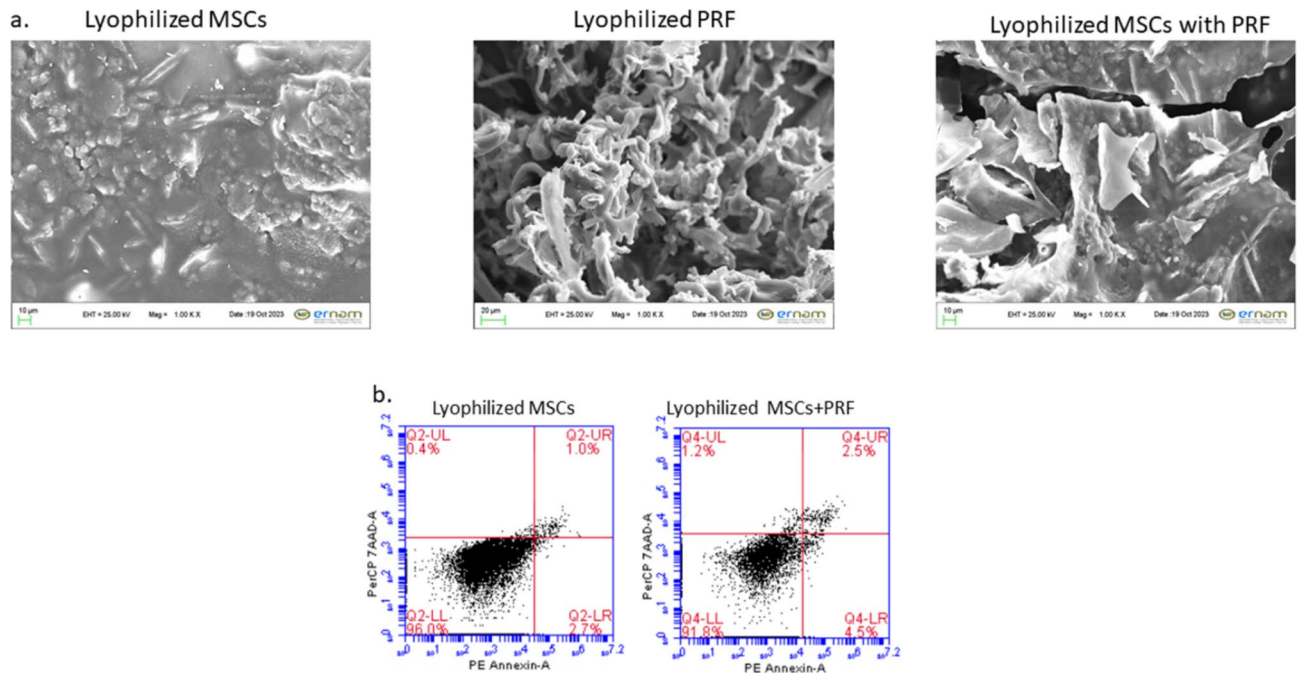


Fig. 1. (a) Scanning electron microscope images of lyophilized DFMSC, lyophilized PRF, and lyophilized DFMSC with PRF. The cells are shown with red arrows. (b) Cell survival analysis of lyophilized MSCs after thawing via flow cytometry. Lower left quadrant: living cells.

analysis via flow cytometry. The lower left quadrant was analyzed for the living cells. The data was presented as the percentage (%) of the cells.

Macroscopic examination of wound healing

To examine wound healing macroscopically for the observation of gross effect, measurements were made in the wound area.

Wound contraction: Percentage of wound area (in X days) = Wound area on day X (mm²) / Wound area on day 0 (mm²) x 100.

Wound healing: Healing Percentage = Healing area on day X (mm²) / Healing area on day 0 (mm²) x 100.

Healing area: Non-healing area compared to the wound area on day 0 (mm²) = Proliferation tissue on day X (mm²) / Wound area on day 0 (mm²) x 100¹⁶.

To evaluate the healing of the wound area, a ruler was placed next to the wound area to facilitate evaluation and photographs were taken. The skin wound surface areas were calculated by transferring the photographs to the "Image J" program in the computer environment. Total wound healing was found by looking at the difference between days in terms of wound areas.

Histopathological analysis

The tissue samples were taken on the 15th day after euthanasia, placed in 10% formaldehyde solution, embedded in paraffin, and 4–5 micron thick sections were prepared. After deparaffinization, the sections were stained with hematoxylin-eosin (Abcam, Cat.No: ab245880, USA) and epithelial cell morphology, tissue integrity, and lymphocytic infiltration were examined. Tissue integrity refers to the preservation of the normal structure and function of the tissue after injury or wounding. It is characterized by the restoration of the tissue architecture without significant fibrosis or scarring. Scoring was done as follows; tissue integrity present:1, absent:0, lymphocytic infiltration/inflammation severe:3, moderate:2, mild:1, absent:0, scarless mature healing present:1, absent:0, epithelialization severe:3, moderate:2, mild:1, absent:0, fibroblastic proliferation severe:3, moderate:2, mild:1, absent:0. One pathologist and one immunologist examined the tissue sections after hematoxylin-eosin staining.

Immunofluorescent labeling

Immunofluorescent labeling was performed to examine epithelial cell regeneration in skin sections. To observe whether MSCs directly participate in tissue repair, tissue sections were labeled with anti-SMA (Abcam, Cat.No: ab5694, USA) for alpha-smooth muscle actin, which is expressed on myofibroblasts, and the nucleus was labeled with DAPI. For α-SMA labeled cells, the secondary antibody Alexa Fluor 488 (green) antibody was used. The distribution of Qdot-labeled MSCs (red fluorescent) in the tissue area was evaluated alongside α-SMA labelled cells under a fluorescent microscope.

Immunohistochemical analyses

The growth factors (FGF, EGF, VEGF) were analyzed by staining tissue sections with anti-FGF (Abcam, Cat. No: ab207321, USA), anti-EGF (Abcam, Cat.No: ab184265, USA) and anti-VEGF (Abcam, Cat.No: ab214424, USA) as previously described¹⁷. EGF is a granular cytoplasmic marker, and VEGF and FGF are membranous and cytoplasmic markers. Briefly, 4 μm thick paraffin sections were mounted on poly-L-lysine slides. The tissue sections were blocked by preincubation with normal serum diluted in PBS (1:30) for 30 min. Primary antibody staining was performed for 24 h overnight, and secondary antibody staining was done for 1 h. The protein expressions were assessed as follows; absent:0, mild:1, moderate:2, marked:3.

Biochemical analysis

In all groups, blood was collected intracardially into tubes without anticoagulant on the 15th day of the study, before euthanasia, and serum was obtained. The levels of interleukin-6 (IL-6) (AD3249Ra, Andy Gene, Beijing, China), Tumor necrosis factor (TNF-α) (E0764Ra, Bioassay Technology Laboratory, Shanghai, China), total antioxidant status (TAOS) (AD3283Ra Andygene, Beijing, China), total oxidant status (TOS) (E1512Ra; Bioassay Technology Laboratory, Shanghai, China), hydroxyproline (HYPR) (EA0040Ra, Bioassay Technology Laboratory, Shanghai, China) in serum samples were measured using a MVGt Lambda Scan 200 ELISA reader (Bio -Tek Instrument, VT) and Rat ELISA kits (Table 1).

Statistical analysis

Data analysis was performed using the GraphPad Prism 8.0 program (GraphPad Software). Data were presented as mean (Mean) ± standard deviation (SD) (minimum-maximum) values in each group. The normality of the variables was assessed using analytical methods (Kolmogorov-Smirnov/Shapiro-Wilk tests). The one-way Analysis of Variance (ANOVA) test was applied for group comparisons of normally distributed variables for biochemical data. Pairwise post-hoc comparisons were conducted using the Tukey test. The Independent T-test (Student T-test) was employed to compare geriatric and young animals. Kruskal-Wallis test was used for pathological scores. For non-normally distributed variables, pairwise comparisons were conducted using the Mann-Whitney U test and evaluated with Bonferroni correction. A P-value of less than 0.05 was considered statistically significant.

Results

DF-MSCs comply with MSCs criteria

DF-MSCs in the third passage were positive for CD29 (98.3 ± 0.7), CD73 (99.4 ± 0.3), CD90 (97.9 ± 0.8), and CD105 (96.0 ± 0.4), and negative for CD14 (0.9 ± 0.4), CD34 (0.7 ± 0.5), CD45 (1.3 ± 0.6), and HLA-DR (0.4 ± 0.3). DF-MSCs were differentiated to three lineages (osteogenic, chondrogenic, and adipogenic).

Analysis of fresh and lyophilized PRF

The platelet count was between 2.8 × 10⁵/μL and 3.4 × 10⁵/μL in fresh PRF. Fresh and lyophilized PRF were analyzed for platelet derived growth factor (PDGF), vascular endothelial growth factor (VEGF), transforming growth factor beta (TGF-β), and fibroblast growth factor 2 (FGF-2) via flow cytometer. PDGF was 46.118 ± 9.873 pg/mL in fresh PRF, and 43.452 ± 12.384 pg/mL in lyophilized PRF. VEGF was 7.019 ± 886 pg/mL in fresh PRF, and 8.238 ± 452 pg/mL in lyophilized PRF. TGF-β was 14.326 ± 2.845 pg/mL in fresh PRF, and 10.453 ± 3.048 pg/mL in lyophilized PRF. FGF-2 was 2.183 ± 746 pg/mL in fresh PRF, and 3.026 ± 256 pg/mL in lyophilized PRF.

		Control	L-PRF	L- DFMSC	L- PRF+DFMSC	P value
TAOS, U/ml	G	0.64 ± 0.06	0.86 ± 0.05	0.71 ± 0.11	0.82 ± 0.10	N.S
	Y	1.31 ± 0.10	1.32 ± 0.06	1.21 ± 0.04	1.30 ± 0.07	N.S
		P < 0.001	P < 0.01	P < 0.01	P < 0.01	N.S
TOS, U/ml	G	4.56 ± 0.20	4.06 ± 0.17	4.60 ± 0.26	4.72 ± 0.11	N.S
	Y	3.19 ± 0.13	3.09 ± 0.23	3.18 ± 0.16	3.05 ± 0.15	N.S
		P < 0.001	P < 0.01	P < 0.001	P < 0.001	N.S
TNF-α ng/L	G	67.11 ± 8.81	79.61 ± 12.47	51.07 ± 7.26	48.09 ± 5.47	N.S
	Y	60.55 ± 3.71	44.95 ± 4.15	67.33 ± 11.92	66.02 ± 11.12	N.S
		0.503	P < 0.05	0.261	0.167	N.S
IL6, ng/L	G	41.63 ± 1.27 ^b	48.19 ± 0.97 ^a	41.85 ± 1.56 ^b	44.23 ± 1.84 ^{ab}	P < 0.01
	Y	32.01 ± 1.06	31.78 ± 1.18	31.4767 ± 2.04	28.99 ± 1.01	N.S
		P < 0.001	P < 0.001	P < 0.01	P < 0.001	N.S
Hypr, ng/ml	G	1.45 ± 0.04 ^b	1.49 ± 0.05 ^b	1.73 ± 0.09 ^a	1.73 ± 0.07 ^a	P < 0.01
	Y	1.79 ± 0.06	1.85 ± 0.06	1.84 ± 0.04	1.91 ± 0.174	N.S
		P < 0.001	P < 0.001	0.319	0.356	N.S

Table 1. The biochemical parameters on the 15th day of the study and their results. ^{a, b}Different letters in the same line are statistically significant (P < 0.05). G geriatric, Y young, TAOS total antioxidant status, TOS total oxidant status, TNF tumor necrosis factor, IL interleukin, Hypr Hydroxyproline. N.S: Not significant.

Mesenchymal stem cells showed viability after rehydration alone or with PRF

After the rehydration process of DF-MSCs combined with PRF, the proportion of living cells was calculated as 85–90% under the microscope. The count of living cells was 83–87% for MSCs alone after the rehydration process. Flow cytometry analysis showed an average of 88.3% ($88.3 \pm 4.9\%$) of living cells after the rehydration process of lyophilized MSCs combined with PRF, and the average of living cells was 89.1% ($89.1 \pm 7.3\%$) for lyophilized MSCs alone (Fig. 1b).

Lyophilized MSCs combined with PRF accelerated wound healing

In both geriatric and young rats, 100% recovery was observed on the 15th day in all trial groups. Macroscopic evaluation of the wound area showed early healing of wounds in treatment groups with lyophilized MSCs and lyophilized MSCs with PRF compared to untreated groups. According to statistical analysis, the wound area (mm²) significantly decreased in young rats (Group 2) compared to geriatric rats (Group 1) ($P < 0.05$). In wound area measurements, on the 3rd day, the wound area in Group 7 decreased significantly compared to Group 1 ($P < 0.05$). Compared to Group 2 rats, the wound area notably decreased in Group 6 (lyophilized MSCs application to young rats) ($P < 0.05$). On the 7th day, the wound area significantly decreased in the rats in Group 3, Group 5, and Group 7 compared to Group 1 ($P < 0.05$), and decreased in the rats in Group 4, Group 6, and Group 8 compared to Group 2 ($P < 0.05$). In the wound area measurements on the 7th day and 15th day, there was a significant decrease in Group 8, Group 4 and Group 6 compared to other groups ($P < 0.05$). The images are given in Fig. 2a.

The recovery rate in young groups has been determined to be higher than that in geriatric animals. In both geriatric and young rats, DF-MSCs application and DF-MSCs with PRF resulted in almost no wound area around the 10th day, indicating the fastest wound healing. Within the first 3 days after the experimental creation of the wound area, it was determined that in geriatric groups, combined applications of DF-MSCs and PRF showed rapid healing compared to those in young rats, while in individual applications. In young rats, similarly, the combination of PRF with DF-MSCs showed a significantly dominant effect in the first 3 days. In addition, the application of lyophilized DF-MSCs with PRF in young rats (Group 8) showed significant decrease in wound area compared to those in geriatric rats (Group 7) ($P < 0.05$), and the application of lyophilized DF-MSCs showed significant decrease in wound area in young rats (Group 6) compared to those in geriatric rats (Group 5) ($P < 0.05$). The results are given in Fig. 2b, and Table 2.

Lyophilized MSCs with PRF achieved scar-free wound healing

Tissue samples were examined for tissue integrity, epithelial regeneration, scarring, inflammatory cells, and fibroblastic proliferation after hematoxylin-eosin staining. In rats in Group 1 and Group 2 (untreated rats), incomplete tissue integrity, granulation tissue, and epithelial loss were observed. Scar-free healing and epithelialization significantly increased in the DF-MSCs with PRF-applied groups (Group 7 and Group 8) compared to the other groups ($P < 0.05$). Tissue integrity was significantly increased in Group 4 (0.6 ± 0.5), Group 5 (0.6 ± 0.5), Group 6 (0.8 ± 0.4), Group 7 (1.0 ± 0.0), and Group 8 (1.0 ± 0.0) compared to Group 1 (0.0 ± 0.0),

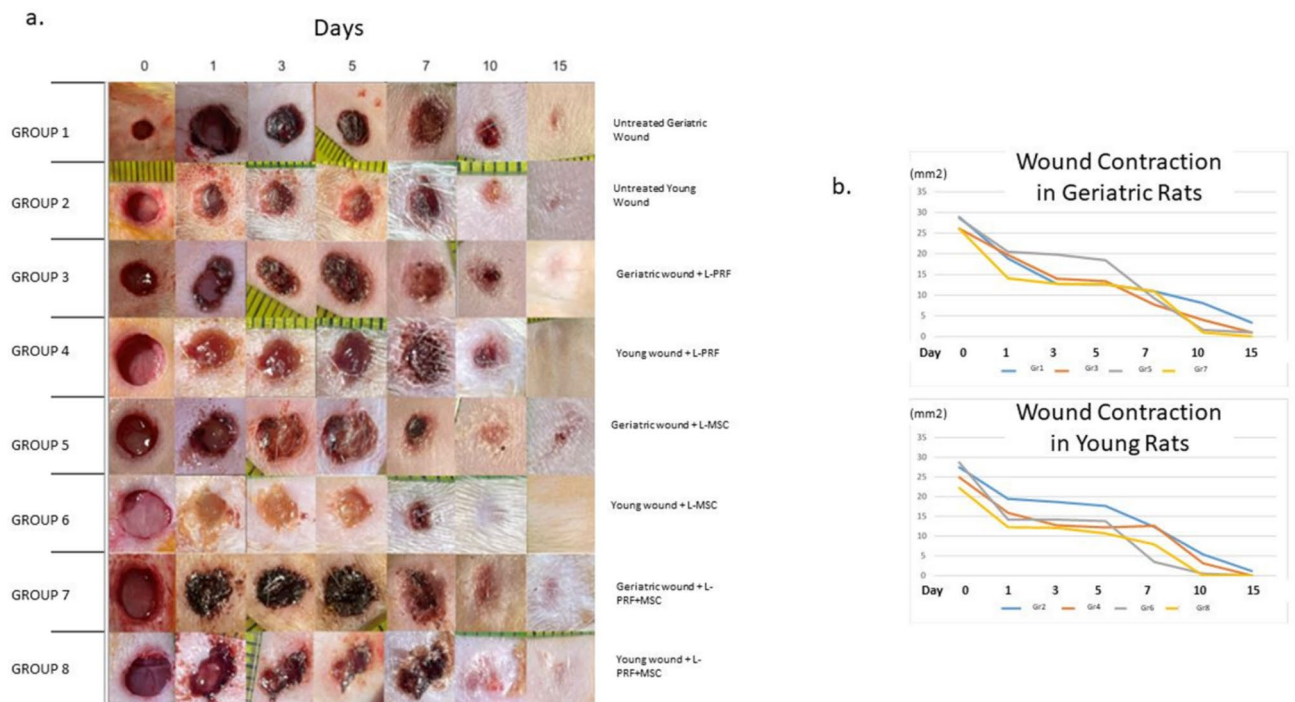


Fig. 2. Macroscopic evaluation of wound healing. (a) Images of wound area beginning from day 0 to day 15. (b) Wound contraction graphics for young and geriatric rats between day 0 and day 15.

Groups	Day 1	Day 3	Day 5	Day 7	Day 10	Day 15
Group 1	19.11 ± 2.81	18.75 ± 2.26	17.04 ± 3.45	12.47 ± 3.61 ^a	6.38 ± 2.11 ^a	1.42 ± 0.61 ^a
Group 2	16.57 ± 3.47	15.26 ± 3.11	13.87 ± 4.23	11.02 ± 3.49 ^{ab}	4.55 ± 2.18 ^b	0.83 ± 0.22 ^b
Group 3	18.16 ± 4.12	15.93 ± 5.38	14.52 ± 2.89	8.27 ± 2.36 ^{bc}	3.60 ± 1.29 ^b	0.76 ± 0.28 ^b
Group 4	15.12 ± 2.29	13.94 ± 1.19	13.20 ± 1.69	8.08 ± 4.12 ^{bc}	1.55 ± 0.27 ^c	0.00 ± 0.00 ^c
Group 5	19.05 ± 3.67	15.16 ± 4.41	15.33 ± 1.76	10.03 ± 1.14 ^a	3.89 ± 1.15 ^b	0.33 ± 0.67 ^c
Group 6	18.93 ± 4.26	16.78 ± 4.81	14.99 ± 5.56	8.12 ± 2.47 ^b	1.65 ± 0.85 ^c	0.00 ± 0.00 ^c
Group 7	18.49 ± 3.96	17.16 ± 2.89	13.86 ± 2.75	7.97 ± 3.06 ^{bc}	1.97 ± 0.76 ^c	0.33 ± 0.67 ^c
Group 8	17.18 ± 4.13	15.65 ± 3.21	14.49 ± 3.28	5.54 ± 1.68 ^c	0.00 ± 0.00 ^d	0.00 ± 0.00 ^c
P value	N.S	N.S	N.S	<i>P</i> < 0.01	<i>P</i> < 0.001	<i>P</i> < 0.001

Table 2. Average wound area values (mm²). ^{a, b, c, d} Different letters in the same column are statistically significant (*P* < 0.05). N.S: Not significant.

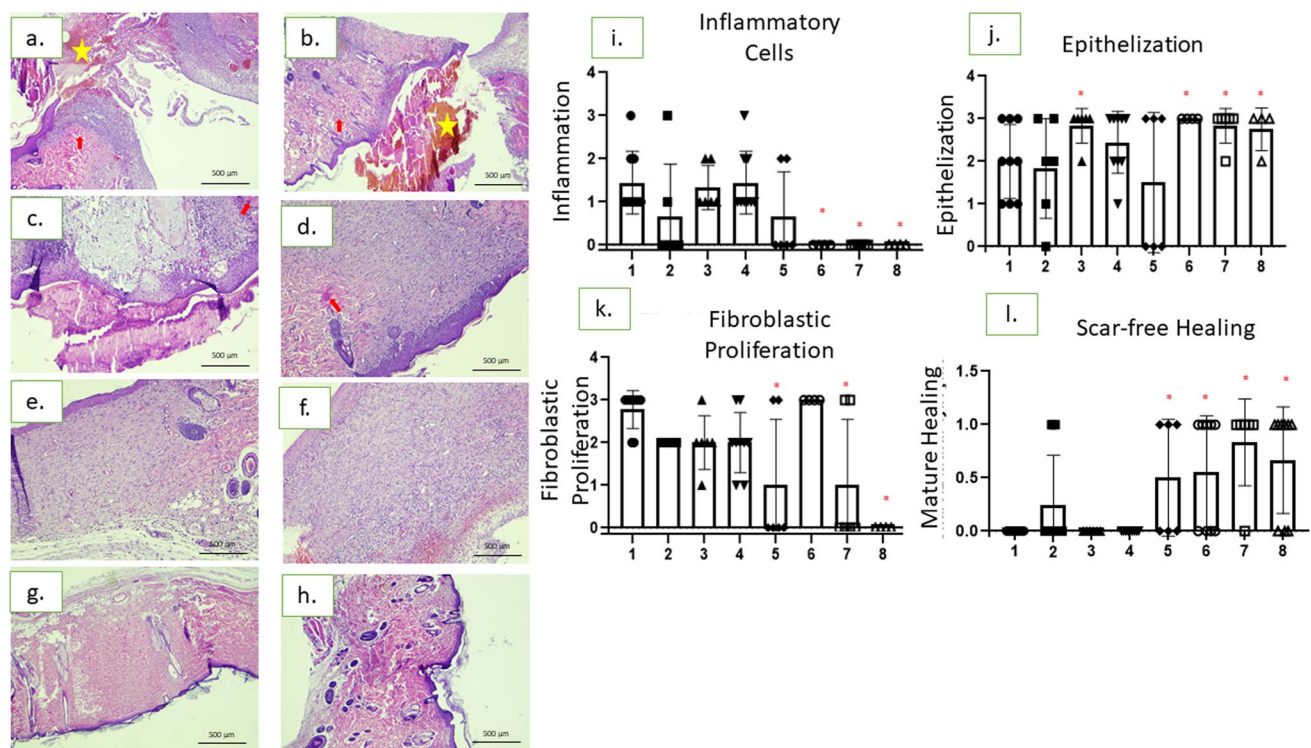


Fig. 3. Histopathological evaluation of wounds at 15 days (x100 magnification). (a) Group 1, loss of tissue integrity, granulation tissue, inflammatory cells, loss of epithelium is observed, (b) Group 2, loss of tissue integrity, granulation tissue, inflammatory cells, the epithelial loss is observed, (c) Group 3, tissue integrity is partial, low epithelialization, (d) Group 4, and (e) Group 5, high rate of epithelialization, tissue integrity is largely maintained, mild granulation tissue, (f) Group 6, high level of epithelialization where tissue integrity is largely maintained, (g) Group 7, complete epithelialization, full tissue integrity, (h) Group 8, full tissue integrity, complete epithelialization was observed with hematoxylin-eosin staining microscope images. (i) Statistical analysis for inflammatory cells scoring. (j) Statistical analysis for epithelization scoring. (k) Statistical analysis for fibroblastic proliferation scoring. (l) Statistical analysis for scar-free healing. Arrows show fibroblastic proliferation, and stars show granulation tissue. In the bar chart red stars indicate the significance, triangles, squares or circles are distribution of individuals. The significance level of study groups is calculated based on SD.

Group 2 (0.2 ± 0.4), Group 3 (0.4 ± 0.5) ($p < 0.05$). Inflammatory cell infiltrate decreased significantly in Group 6, Group 7, and Group 8 compared to the other groups ($P < 0.05$). Fibroblastic proliferation decreased significantly in Group 5, Group 7, and Group 8 compared to other groups ($P < 0.05$). Scar free healing was significant in Group 5, Group 6, Group 7, and Group 8 ($P < 0.05$). The results may prove that lyophilized DF-MSCs may have a regenerative effect as well as a regulatory effect on the inflammatory process in wound tissue. In addition, the application of lyophilized DF-MSCs with PRF not only reduces the inflammatory infiltrate but also supports scar-free healing (Fig. 3).

Lyophilized DF-MSCs contributed to epithelial regeneration at the wound site

To determine whether lyophilized DF-MSCs directly participates in tissue repair, tissue sections were labeled with anti-SMA for alpha-smooth muscle actin, which is co-expressed on epithelial cells. The distribution of Qdot labeled DF-MSCs (red) in the tissue sections was evaluated under a fluorescent microscope. The rate of Qdot⁺SMA⁺ cells was found to be $52.7 \pm 8.3\%$ in Group 5, while it was $48.4 \pm 7.1\%$ in Group 7. The ratio of Qdot⁺SMA⁺ cells was found to be $53.2 \pm 6.4\%$ in Group 6 while the ratio of Qdot⁺SMA⁺ cells was $51.8 \pm 5.9\%$ in Group 8. According to the results, lyophilized DF-MSC contributes to epithelial regeneration in the wound area (Fig. 4).

Lyophilized DF-MSCs with PRF synergistically increased VEGF expression

MSCs can also contribute to the regeneration of the wound area by increasing the secretion of EGF, and FGF growth factors from other tissue cells¹⁸. In this study, we analyzed the expression of growth factors in geriatric groups with difficult wound healing. The results of immunohistochemical staining demonstrated that lyophilized DF-MSCs significantly decreased the expression of FGF in Group 5 (0.4 ± 0.6), and Group 7 (0.2 ± 0.3) compared to untreated (Group 1: 1.2 ± 0.8) and lyophilized PRF treatment group (Group 3: 1.2 ± 0.8) ($P < 0.05$). The expression of EGF notably increased in Group 5 (1.2 ± 0.8), and Group 7 (1.4 ± 0.6) compared to the untreated (Group 1: 0.6 ± 0.4) and lyophilized PRF treatment group (Group 3: 0.2 ± 0.6) ($P < 0.05$). VEGF expression was significantly increased in Group 3 (0.7 ± 0.8), Group 5 (1.3 ± 0.5), and Group 7 (1.3 ± 0.5) compared to Group 1 (0.0 ± 0.0) ($P < 0.05$). The expression of VEGF was significantly high in Group 7 when compared with Group 3 and Group 5 ($P < 0.05$). Lyophilized DF-MSCs alone and in combination with PRF significantly decreased the

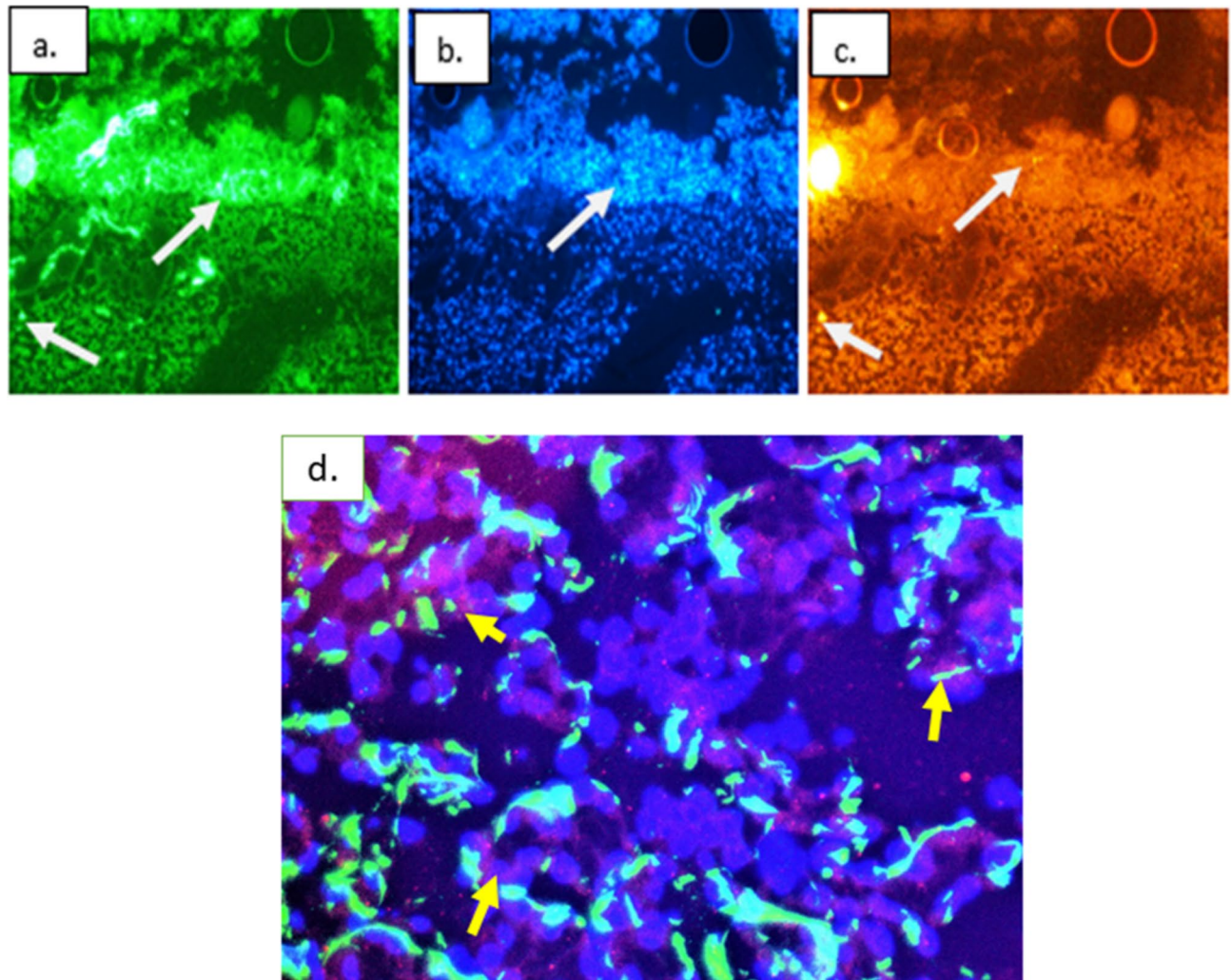


Fig. 4. Fluorescent microscope image of Qdot labeled cells expressing α -SMA in the skin section. (a) In the tissue section labeled with α -SMA antibody, cells expressing α -SMA are seen in green. (b) After staining the cell nucleus with DAPI, the blue nucleus appears in the tissue section. (c) The image of Qdot labeled cells in the tissue section appears bright red/bright orange (x200 magnification). (d) The merged image of Qdot-labeled cells expressing α -SMA in a skin section (x1000 magnification). Fluorescence microscope intensity analysis of the cells shows that Qdot labeled cells express α -SMA at an average rate of 58%.

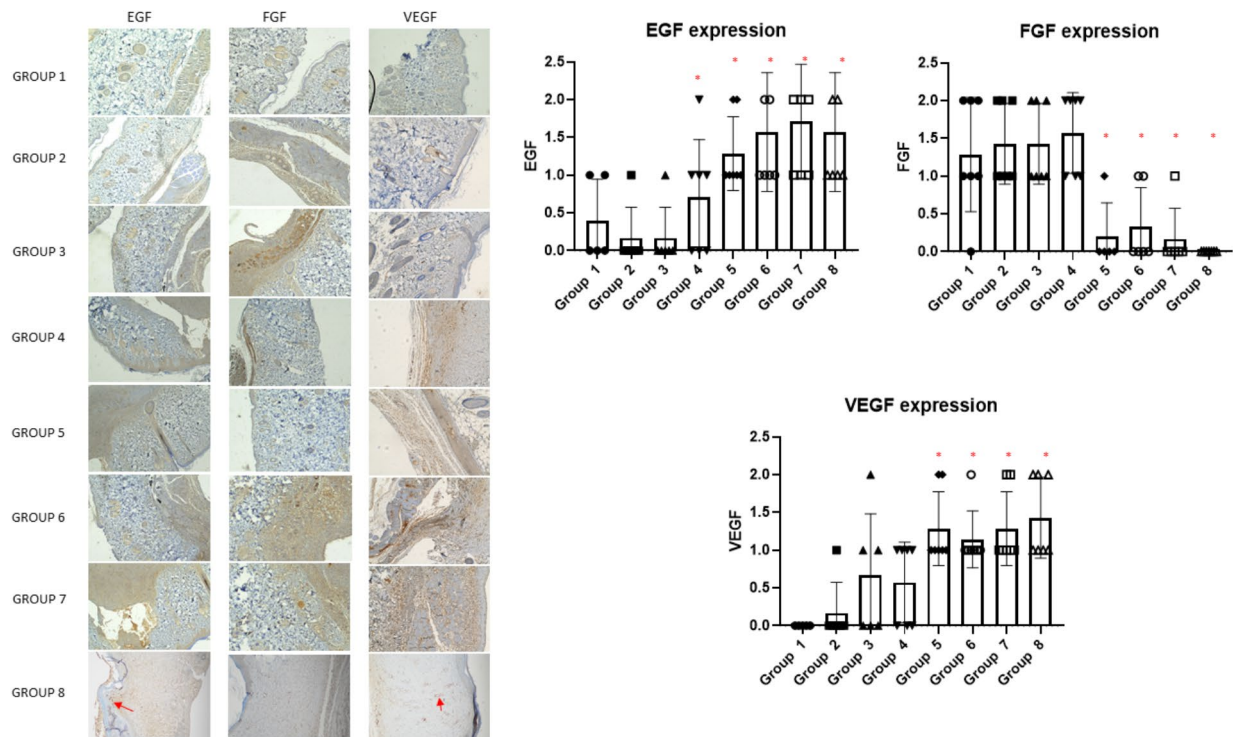


Fig. 5. Immunohistochemical staining (15th day) (x100 magnification). The EGF and VEGF expressions significantly increased (red arrows) and FGF expression notably downregulated in geriatric rats treated with lyophilized PRF and MSCs.

expression of FGF in Group 6 (0.6 ± 0.6), and Group 8 (0.0 ± 0.0) compared to untreated (Group 2: 1.4 ± 0.6) and lyophilized PRF treatment group (Group 3: 1.2 ± 0.8) ($P < 0.05$). The expression of EGF significantly increased in Group 4 (0.7 ± 0.6), Group 6 (1.6 ± 0.7), and Group 8 (1.7 ± 0.6) compared to the untreated (Group 2: 0.2 ± 0.4) ($P < 0.05$). The expression of VEGF significantly increased in Group 6 (1.1 ± 0.3) and Group 8 (1.4 ± 0.6) when compared with Group 2 (0.2 ± 0.4) and Group 4 (0.5 ± 0.6) ($P < 0.05$). The data indicate that DF-MSCs with PRF may have a synergic effect on VEGF expression (Fig. 5).

Biochemical analysis results

On the 15th day, in geriatric rats, hydroxyproline levels increased in the DF-MSCs and DF-MSCs with PRF groups ($P < 0.01$), and IL6 increased in the PRF group compared to the control group ($P < 0.01$). No differences were found among groups in TAOS and TOS values in geriatric rats ($P < 0.05$). Furthermore, in geriatric rats, TNF was found to increase in the PRF group compared to the DF-MSCs and PRF + DF-MSCs groups ($P < 0.05$). In the control group, geriatric rats exhibited lower serum hydroxyproline and TAOS levels ($P < 0.001$) and higher TOS and IL6 levels ($P < 0.001$) compared to young rats. However, no difference was observed in hydroxyproline levels between young and geriatric animals in the MSC and PRF + MSC groups ($P < 0.05$). Additionally, TNF was found to be higher in the PRF group in geriatric rats compared to young rats ($P < 0.05$). The results are given in the Table 1.

Discussion

In this study, PRF and MSCs, known to contribute to the healing process in cutaneous wounds, were lyophilized to obtain a shelf-stable product. The effect of lyophilized MSCs with PRF on the regeneration process was investigated by applying it to traumatic cutaneous wounds created in geriatric rats, which are difficult to heal. These results were then compared with the wound healing in young rats. The results of the present study demonstrated that cutaneous wounds in geriatric rats healed slower than in young rats. However, the topical application of lyophilized DF-MSCs alone or with PRF promoted wound healing in geriatric rats to a level similar to that in young rats. In this study, rat PRF was used for lyophilization of human DF-MSCs, as lyophilized PRF alone or together with DF-MSCs was used in rat skin wounds to avoid causing hypersensitivity reaction between different species.

MSCs are promising cell types for clinical applications due to their ability to differentiate into multiple cell types¹⁹, however the most common challenge of MSCs in clinical applications is the freezing, thawing, and transportation of the cells²⁰. Therefore, there is still a need for the production of MSCs in a shelf-stable form that will enable their rapid use in clinical applications.

PRF is a fibrin matrix that can act as a resorbable membrane. This membrane retains platelet cytokines, growth factors, and cells²¹. Additionally, PRF can promote the survival and regenerative capacity of MSCs, creating a protective microenvironment for MSCs *ex vivo*²².

Trehalose is a non-toxic disaccharide composed of two molecules of glucose. It is known that MSCs can be protected from freezing, dehydration, or other environmental conditions by loading them with trehalose¹⁴. In the present study, we aimed to prepare MSCs with a new combination as a therapeutic agent for skin wounds, preserving their viability and functionality while also keeping them in a shelf-stable state. Therefore, as a new methodology, we incubated MSCs with PRF for 1–2 h at 37 °C and then mixed with 100 mM trehalose before freeze-drying.

In this study, we observed that the healing of lyophilized DF-MSCs applied to the wound area in both geriatric and young rats was rapid when combined with PRF with increased epithelialization, tissue integrity, and scar-free healing in the wound area. Therefore, we investigated the regeneration mechanism of lyophilized DF-MSCs and PRF by analyzing fluorescently labeled cells and growth factors in wound tissue. The fluorescent-labeled lyophilized DF-MSCs differentiated into epithelial cells at a ratio of 48–53%. In previous studies, it was reported that freshly prepared MSCs can differentiate into non-mesodermal cell types such as epithelial, hepatocyte, and renal tubular cells^{23,24}. The data showed that lyophilized DF-MSCs can differentiate to epithelial cells after being transferred to the wound site.

MSCs facilitate the regeneration of damaged tissue largely with the growth factors they secrete²⁵. FGF, a tissue regenerative mediator, is also secreted by MSCs and tissue cells at the wound site by triggering the activation of alternative macrophages and fibroblasts that play a role in tissue regeneration²⁶. FGF is an immature healing marker for wound healing. In a scar-free healing as healing is completed, fibroblasts decrease since they return to normal tissue volume²⁶. EGF has been shown to induce the differentiation of MSCs into dermal cells and increase the wound healing rate^{27,28}. VEGF stimulates angiogenesis at the wound site and also affects wound closure and epidermal repair, granulation tissue formation, both in terms of the strength of the healing wound and the amount of scar tissue accumulated²⁸. In this study, lyophilized DF-MSCs increased the expressions of VEGF and EGF at the wound site in groups treated with lyophilized MSCs. The expressions of FGF or EGF were similar in the lyophilized DF-MSCs and DF-MSCs with PRF groups, but the expression of VEGF or EGF did not change in the lyophilized PRF alone groups. Data show that lyophilized MSCs can secrete growth factors, thereby accelerating wound healing. Interestingly, lyophilized PRF was tended to increase VEGF expression at the wound site, but VEGF expression was further increased by the application of DF-MSCs with PRF. These data indicate the synergistic effect of lyophilized DF-MSC and PRF on wound healing.

An increase or decrease in TOS and TAOS can significantly impact wound healing. Increase in TOS leads to higher oxidative stress, causing tissue damage, delayed healing, and prolonged inflammation, which interferes with fibroblast activity and collagen synthesis. Decrease in TOS reduces oxidative stress, promoting faster tissue repair, balanced inflammation, and smoother wound healing. Increase in TAOS boosts antioxidant defenses, protecting cells, enhancing tissue regeneration, and reducing chronic inflammation, supporting quicker recovery. Decrease in TAOS weakens antioxidant defenses, leading to more oxidative damage, slowed healing, and a higher risk of chronic, non-healing wounds. The balance between TOS and TAOS is critical for efficient wound healing. Elevated TOS can delay or complicate healing, while higher TAOS supports recovery by mitigating oxidative stress²⁹. In this study, it was observed that the serum TOS level of geriatric rats increased in all groups, while the TAOS level decreased, thus increasing oxidative stress. It was determined that PRF and MSC applications did not have effect on TOS and TAOS. Oxidative stress occurs when there is an imbalance between the concentration of reactive oxygen species (ROS) and the capacity of the antioxidative system to neutralize ROS. Aging and cellular senescence are characterized by prolonged activation of inflammatory pathways and increased oxidative stress^{30,31}. It has been observed that as cells age, they sustain more DNA damage from oxidants^{32,33}. IL-6 is essential in both initiating and resolving inflammation, promoting fibroblast activity and angiogenesis, and aiding in tissue regeneration. TNF- α , while crucial for the initial inflammatory response and pathogen clearance, can lead to chronic inflammation and fibrosis if uncontrolled, negatively impacting wound healing. Together, these cytokines are critical regulators of the wound healing process, with IL-6 favoring repair and regeneration, while TNF- α can complicate healing if not properly balanced³⁴. In this study, serum IL6 and TNF levels increased in geriatric rats. Cytokines are produced by various cell types, such as macrophages, platelets, and keratinocytes. They mediate many functions, including the initiation or influence of many biological processes such as inflammation and wound healing^{33,35}. PRF has been shown in numerous studies to have substantial anti-inflammatory properties³⁶. The rise in TNF- α and IL-6 after PRF application reflects the activation of the inflammatory phase, which is necessary for wound healing. The additional increase in IL-6 in the combination group suggests a complex interplay where both inflammation and regeneration are being actively promoted, especially important in the context of geriatric healing, where immune function is often compromised^{13,37}. The results of this study demonstrated that PRF application in geriatric rats increased the levels of TNF and IL6. Although allogeneic PRF is recommended to be used, especially in wound treatment, it is reported that more research is needed regarding its safety³⁶. Presumably, the allogeneic nature of the PRF used in this study caused an increase in IL6 and TNF levels in geriatric animals.

The aging process exerts a detrimental influence on the typical mechanisms involved in wound healing. The extracellular matrix undergoes structural and functional changes with age, along with alterations in the release of growth factors. These changes play a role in the development of chronic wounds³⁸. Aged skin has reduced collagen synthesis and the breakdown of collagen generates free HYPR^{39,40}. HYPR levels serve as an important indicator of the state of collagen metabolism in the wound healing process, with increased levels signifying collagen breakdown and decreased levels suggesting a shift towards repair and new collagen formation⁴¹. Similar to prior investigations, the HYPR level in the geriatric control group was lower than that of the young group. Nevertheless, the serum HYPR level increased following the treatment with DF-MSCs and DF-MSCs with PRF.

These results suggested that the lyophilized MSC used in the current study might encourage wound healing by stimulating collagen synthesis in the tissue.

In addition, the lyophilization process is the removal of the water content of the cells to preserve the cells dry for a long time. Quantum dot (Qdot) nanoparticles can also be preserved for a long time by freeze-drying^{40,42}. In vivo observations in this study showed that MSCs can also contain Qdot fluorescent nanoparticles after the lyophilization process. According to our results, it has been observed that Qdot labeled cells before lyophilization for tracking MSCs in vivo can still provide fluorescence in the tissue. These results may indicate that lyophilized cells do not lose the fluorescent nanoparticles they contain, as reported by the previous studies^{42,43}. There are various methods for lyophilization of cells; some contain only disaccharides such as trehalose or sucrose, or serum albumin or combinations of similar ingredients⁴³. However, there are few studies on freeze-dried MSCs. In a study, lyophilized administration of human umbilical cord MSCs with a solution containing PVP, trehalose, and sucrose resulted in increased vascular regeneration but resulted in thrombus formation, morphological changes, and inflammation⁴⁴. For this reason, the lyophilization process is important in keeping the cells without losing their functionality.

Secretory products of MSCs can heal the wound, but MSCs are important in the healing process as they carry out tissue regeneration through cell-cell contact. Additionally, MSCs can accelerate the healing process by differentiating into other cells in the wound⁴⁵. Therefore, the viability and differentiation or tissue regeneration ability of the cells must be preserved after the lyophilization process. In this study, the experimental results of the formulation we developed for the lyophilization of MSCs show that the differentiation abilities of MSCs and their functionality in secreting paracrine factors required for tissue repair are preserved.

Conclusions

The main purpose of this study was to investigate the effects of lyophilized MSCs in the skin wound niche. Skin wounds have a microenvironment composed of inflammatory cells such as macrophages, neutrophils, lymphocytes, injured epithelium, and exudates containing proteinaceous fluid^{9,46–48}. On the other hand, we analyzed MSCs for cell survival after lyophilization by dissolving them in a DMEM medium to simulate an aqueous environment. The analysis showed that the lyophilized cells were able to return to a living state by gaining cytoplasm and continuing to heal the wound. Therefore, lyophilized MSCs shown to be not destroyed after the lyophilization process.

In conclusion, while lyophilized MSCs alone can accelerate wound healing in geriatric rats, their application in combination with PRF further increases the healing rate. Moreover, lyophilized MSCs maintain their viability and functionality for wound healing when freeze-dried in combination with PRF.

Data availability

The datasets used and/or analysed during the current study available from the corresponding author on reasonable request.

Received: 3 June 2024; Accepted: 1 January 2025

Published online: 24 February 2025

References

- Kössi, J., Elenius, K., Niinikoski, J., Peltonen, J. & Laato, M. Overview of wound healing. *Ann. Chir. Gynaecol.* **215**, 15–18 (2001).
- Le Blanc, J. & Lordkipanidzé, M. Platelet function in aging. *Front. Cardiovasc. Med.* **6**, 109 (2019).
- Lin, C. S., Lin, G. & Lue, T. F. Allogeneic and xenogeneic transplantation of adipose-derived stem cells in immunocompetent recipients without immunosuppressants. *Stem Cells Dev.* **21**, 2770–2778 (2012).
- Graca, M. F., Miguel, S. P., Cabral, C. S. & Correia, I. J. Hyaluronic acid-based wound dressings: A review. *Carbohydr. Polym.* **241**, 116364 (2020).
- Dave, J. R. & Tomar, G. B. Dental tissue-derived mesenchymal stem cells: Applications in tissue engineering. *Crit. Rev. Biomed. Eng.* **46**, 429–68 (2018).
- Khurana, R., Kudva, P. B. & Husain, S. Y. Comparative evaluation of the isolation and quantification of stem cells derived from dental pulp and periodontal ligament of a permanent tooth and to assess their viability and proliferation on a platelet-rich fibrin scaffold. *J. Indian Soc. Periodontol.* **21**, 16–20 (2017).
- Ngah, N. A. et al. Lyophilised platelet-rich fibrin: Physical and biological characterisation. *Molecules* **26**, 7131 (2021).
- Narayanaswamy, R. et al. Evolution and clinical advances of platelet-rich fibrin in musculoskeletal regeneration. *Bioengineering (Basel)* **10**, 58 (2023).
- Maxson, S., Lopez, E. A., Yoo, D., Danilkovitch-Miagkova, A. & Leroux, M. A. Concise review: Role of mesenchymal stem cells in wound repair. *Stem Cells Transl. Med.* **1**, 142–149 (2012).
- Lin, W. et al. Mesenchymal stem cells homing to improve bone healing. *J. Orthop. Translat.* **29**, 19–27 (2017).
- Li, Q. et al. Lyophilized platelet-rich fibrin (PRF) promotes craniofacial bone regeneration through Runx2. *Int. J. Mol. Sci.* **15**, 8509–8525 (2014).
- Nilay Tutak, F. & Annaç, E. The effect of mesenchymal stem cells lyophilisate femoral artery of rat anastomosis: A histopathological and histomorphometric study. *Ann. Med. Surg. (Lond.)* **70**, 102861 (2021).
- Toruntay Cin, G., Lektemur Alpan, A. & Çevik, Ö. Efficacy of injectable platelet-rich fibrin on clinical and biochemical parameters in non-surgical periodontal treatment: A split-mouth randomized controlled trial. *Clin. Oral. Invest.* **28**, 46 (2024).
- Zhang, S. Z. et al. Preliminary study on the freeze-drying of human bone marrow-derived mesenchymal stem cells. *J. Zhejiang Univ. Sci. B.* **11**, 889–894 (2010).
- Murthy, S. et al. Evaluation of in vivo wound healing activity of *Bacopa monniera* on different wound model in rats. *Biomed. Res. Int.* **2013**, 972028 (2013).
- Sabol, F. et al. Immunohistological changes in skin wounds during the early periods of healing in a rat model. *Vet. Med. Czech.* **57**, 77–82 (2012).
- De Araújo Farias, V., Carrillo-Gálvez, A. B., Martín, F. & Anderson, P. TGF- β and mesenchymal stromal cells in regenerative medicine, autoimmunity and cancer. *Cytokine Growth Factor Rev.* **43**, 25–37 (2018).

18. Ayala-Cuellar, A. P., Kang, J. H., Jeung, E. B. & Choi, K. C. Roles of mesenchymal stem cells in tissue regeneration and immunomodulation. *Biomol. Ther. (Seoul)* **27**, 25–33 (2019).
19. Linkova, D. D., Rubtsova, Y. P. & Egorikhina, M. N. Cryostorage of mesenchymal stem cells and biomedical cell-based products. *Cells* **11**, 2691 (2022).
20. Bilgen, F., Ural, A. & Bekerecioglu, M. Platelet-rich fibrin: An effective chronic wound healing accelerator. *J. Tissue Viability* **30**, 616–620 (2021).
21. Desposito, V. et al. Platelet-rich plasma increases growth and motility of adipose tissue-derived mesenchymal stem cells and controls adipocyte secretory function. *J. Cell Biochem.* **116**, 2408–24018 (2015).
22. Quinn, C. & Flake, A. W. In vivo differentiation potential of mesenchymal stem cells: Prenatal and postnatal model systems. *Transfus. Med. Hemother.* **35**, 239–247 (2008).
23. Genç, D. et al. Dental follicle mesenchymal stem cells ameliorated glandular dysfunction in Sjögren's syndrome murine model. *PLoS One* **17**, e0266137 (2022).
24. Lee, D. E., Ayoub, N. & Agrawal, D. K. Mesenchymal stem cells and cutaneous wound healing: Novel methods to increase cell delivery and therapeutic efficacy. *Stem Cell Res. Ther.* **9**, 37 (2016).
25. Lu, D., Xu, Y., Liu, Q. & Zhang, Q. Mesenchymal stem cell-macrophage crosstalk and maintenance of inflammatory microenvironment homeostasis. *Front. Cell Dev. Biol.* **9**, 681171 (2021).
26. Fierro, F. A., Kalomoiris, S., Sondergaard, C. S. & Nolta, J. A. Effects on proliferation and differentiation of multipotent bone marrow stromal cells engineered to express growth factors for combined cell and gene therapy. *Stem Cells* **29**, 1727–1737 (2011).
27. Xia, Y. et al. Epidermal growth factor promotes mesenchymal stem cell-mediated wound healing and hair follicle regeneration. *Int. J. Clin. Exp. Pathol.* **10**, 7390–7400 (2017).
28. Demidova-Rice, T. N., Hamblin, M. R. & Herman, I. M. Acute and impaired wound healing: Pathophysiology and current methods for drug delivery, part 2: Role of growth factors in normal and pathological wound healing: Therapeutic potential and methods of delivery. *Adv. Skin. Wound Care.* **25**, 349–370 (2012).
29. Sies, H. Oxidative stress: A concept in redox biology and medicine. *Redox Biol.* **4**, 180–183 (2015).
30. Varga-Medveczky, Z. et al. Age-related inflammatory balance shift, nasal barrier function, and cerebro-morphological status in healthy and diseased rodents. *Front. Neurosci.* **15**, 700729 (2021).
31. Jin, K. Modern biological theories of aging. *Aging Dis.* **1**, 72–74 (2010).
32. Zuo, L. et al. Inflammaging and oxidative stress in human diseases: From molecular mechanisms to novel treatments. *Int. J. Mol. Sci.* **20**, 4472 (2019).
33. Fernández-Guarino, M., Hernández-Bule, M. L. & Bacci, S. Cellular and molecular processes in wound healing. *Biomedicines* **11**, 2526 (2023).
34. Eming, S. A., Wynn, T. A. & Martin, P. Inflammation and metabolism in tissue repair and regeneration. *Science* **356**, 1026–1030 (2017).
35. Johnson, B. Z., Stevenson, A. W., Prêle, C. M., Fear, M. W. & Wood, F. M. The role of IL-6 in skin fibrosis and cutaneous wound healing. *Biomedicines* **8**, 101 (2020).
36. Kargarpour, Z., Panahipour, L., Mildner, M., Miron, R. J. & Gruber, R. Lipids of platelet-rich fibrin reduce the inflammatory response in mesenchymal cells and macrophages. *Cells* **12**, 634 (2023).
37. Abdel-Salam, B. K. A. H. Modulatory effect of whey proteins in some cytokines involved in wound healing in male diabetic albino rats. *Inflammation* **37**, 1616–1622 (2014).
38. Naik, B., Karunakar, P., Jayadev, M. & Marshal, V. R. Role of platelet rich fibrin in wound healing: A critical review. *J. Conserv. Dent.* **16**, 284–293 (2013).
39. Diller, R. B. & Tabor, A. J. The role of the extracellular matrix (ECM) in wound healing: A review. *Biomimetics (Basel)* **7**, 87 (2022).
40. Ding, X., Kakanj, P., Leptin, M. & Eming, S. A. Regulation of the wound healing response during aging. *J. Invest. Dermatol.* **141**, 1063–1070 (2021).
41. Vater, C., Kasten, P. & Stiehler, M. Culture media for the differentiation of mesenchymal stromal cells. *Acta Biomaterialia* **7**, 463–477 (2011).
42. Cissell, D. D., Link, J. M., Hu, J. C. & Athanasiou, K. A. A modified hydroxyproline assay based on hydrochloric acid in ehrlich's solution accurately measures tissue collagen content. *Tissue Eng. Part C Methods* **23**, 243–250 (2017).
43. Jimi, S. et al. Acceleration mechanisms of skin wound healing by autologous micrograft in mice. *Int. J. Mol. Sci.* **18**, 1675 (2017).
44. Gatto, M. S. & Najahi-Missaoui, W. Lyophilization of nanoparticles, does it really work? Overview of the current status and challenges. *Int. J. Mol. Sci.* **24**, 14041 (2023).
45. Gofman, V. V. et al. Freeze-dried polymer-coated quantum dots for perspective biomedical application. In *Saratov Fall Meeting 2014: Optical Technologies in Biophysics and Medicine XVI; Laser Physics and Photonics XVI; and Computational Biophysics*. Vol. 9448. SPIE, (2015).
46. Paresishvili, T. & Kakabadze, Z. Freeze-dried mesenchymal stem cells: From bench to bedside. *Rev. Adv. Biol.* **8**, 2300155 (2024).
47. Tutak, F. N. & Annaç, E. The effect of mesenchymal stem cells lyophilisate on femoral artery of rat anastomosis: A histopathological and histomorphometric study. *Ann. Med. Sur.* **70**, 102861 (2021).
48. Maxson, S., Lopez, E. A., Yoo, D., Danilkovitch-Miagkova, A. & Leroux, M. A. Concise review: Role of mesenchymal stem cells in wound repair. *Stem Cells Transl. Med.* **1**, 142–149 (2012).
49. Wang, Z., Qi, F., Luo, H., Xu, G. & Wang, D. Inflammatory microenvironment of skin wounds. *Front. Immunol.* **13**, 789274 (2022).

Acknowledgments

This study is supported by THE SCIENTIFIC AND TECHNOLOGICAL RESEARCH COUNCIL OF TÜRKİYE (TUBITAK) with project number 122O688.

Author contributions

O.B. and D.G. designed the study. O.B. and T.M.D. conducted the experiments. O.B. and D.G. acquired the data. O.B. D.G. Ç.E.D. L.T. A.B. analyzed the data. D.G. Ç.E.D. L.T. A.B. contributed the reagents and materials. O.B. D.G. L.T. and A.B. wrote the manuscript.

Declarations

Competing interests

The authors declare no competing interests.

Additional information

Supplementary Information The online version contains supplementary material available at <https://doi.org/10.1038/s41598-025-85238-1>.

Correspondence and requests for materials should be addressed to O.B.

Reprints and permissions information is available at www.nature.com/reprints.

Publisher's note Springer Nature remains neutral with regard to jurisdictional claims in published maps and institutional affiliations.

Open Access This article is licensed under a Creative Commons Attribution-NonCommercial-NoDerivatives 4.0 International License, which permits any non-commercial use, sharing, distribution and reproduction in any medium or format, as long as you give appropriate credit to the original author(s) and the source, provide a link to the Creative Commons licence, and indicate if you modified the licensed material. You do not have permission under this licence to share adapted material derived from this article or parts of it. The images or other third party material in this article are included in the article's Creative Commons licence, unless indicated otherwise in a credit line to the material. If material is not included in the article's Creative Commons licence and your intended use is not permitted by statutory regulation or exceeds the permitted use, you will need to obtain permission directly from the copyright holder. To view a copy of this licence, visit <http://creativecommons.org/licenses/by-nc-nd/4.0/>.

© The Author(s) 2025